STRUCTURAL PROPERTY OF ALH_3 NANOPARTICLES SYNTHESISED VIA MECHANOCHEMICAL TECHNIQUE

J.A. Murshidi

Malaysian Nuclear Agency (Nuclear Malaysia) Bangi, 43000 Kajang, Selangor, Malaysia
e-mail: julie@nm.gov.my

ABSTRACT

Research into materials based hydrogen storage has grown significantly over the past decade. Of the wide variety of materials based hydrogen storage, AlH_3 nanoparticles were chosen as the primary focus of this paper. AlH_3 nanoparticles were synthesised by mechanochemical reactions of the $3LiAlH_4 + AlCl_3$ using different $LiCl:AlH_3$ volume ratios (0.76:1, 2:1, 5:1 and 10:1) at 77 K. The addition of LiCl as a buffer leads to the reduction of the synthesized AlH_3 crystallite size and preventing high Al yields. Quantitative Rietveld results suggest the presence of an amorphous AlH_3 phase in mechanochemically synthesized samples.

ABSTRAK

Penyelidikan ke dalam simpanan hidrogen berasaskan bahan telah berkembang dengan ketara sepanjang dekad yang lalu. Daripada pelbagai jenis penyimpanan hidrogen berasaskan bahan, nanozarah AlH_3 telah dipilih sebagai fokus utama kertas ini. Nanozarah AlH_3 disintesis melalui tindak balas mekanokimia $3LiAlH_4 + AlCl_3$ menggunakan nisbah isipadu $LiCl:AlH_3$ yang berbeza (0.76:1, 2:1, 5:1 dan 10:1) pada 77 K. Penambahan LiCl sebagai penimbal membawa kepada pengurangan saiz kristal AlH_3 yang disintesis dan menghalang hasil Al yang tinggi. Keputusan Rietveld kuantitatif mencadangkan kehadiran fasa AlH3 amorf dalam sampel yang disintesis secara mekanokimia.

Keywords: Aluminium trihydride, mechanochemical, phase, crystallite size

INTRODUCTION

Many techniques have been developed for the synthesis of nanoparticles including vapor, liquid and solid-state approaches [1,2,3,4]. The solid-state approach takes place by mechanical milling, mechanical alloying, mechanochemical and cryomilling. Herein the mechanochemical and cryomilling techniques are utilised for synthesising aluminium trihydride (AlH_3) nanoparticles.

AlH_3 is a metastable, crystalline solid with a volumetric hydrogen density of 0.148 kg H_2/L and a gravimetric hydrogen density of 10.1 wt%. It has been used as a reducing agent, explosive, rocket fuel, hydrogen source for portable power system, military applications, and automotive applications [5,6]. The mechanochemical technique for synthesizing AlH_3 at room temperature resulted in a mixture of α-AlH_3, α'-AlH_3 and Al phases [7,8,9], showing that mechanochemical milling at room temperature can provides more than enough energy to allow AlH_3 to release hydrogen and form aluminium metal nanoparticles. The number of AlH_3 phases can be controlled by using different ball to powder ratios, ball sizes, milling temperature and milling time [7,8,9]. Approximately 50% of the synthesised AlH_3 decomposes to Al during the first hour of milling when higher ball to powder ratio and larger balls were used [8]. The number of AlH_3 phases was reported to decrease with increased milling time [8,9].

The cryomilling technique originally evolved as a variation of mechanical milling and involves putting the milling media in liquid nitrogen (approximately 77K), and using processing parameters in order to gain nanostructured

particles. The advantages of using cryomilling compared with milling at room temperature is that the extremely low temperature of liquid nitrogen will suppresses recovery and recrystallization and leads to finer grain structures and more rapid grain refinement [10]. Cryomilling forms high AlH_3 yields and minimises the decomposition of AlH_3 to Al compared to room temperature milling [8]. AlH_3has also been reported to form by cryomilling alanate and aluminium halides or by adding additives [9]. Another study shows that the α'-AlH_3 phase synthesized from cryomilling decomposes either partially by a single reaction step or by two decomposition steps [9,11].

A buffer, often the by-product of the reaction, was added to the starting reagents during the mechanochemical reaction in order to control the particle size distribution, to prevent their subsequent growth and suppress their agglomeration. Removal of the buffer was usually carried out through a solvent dissolution technique followed by solid-liquid separation (washing) [12-16]. In order to understand the effect of different buffer quantities on the structural property of AlH_3 nanoparticles, samples were milled for 30 minutes with different LiCl: AlH_3 volume ratios of 0.76:1, 2:1, 5:1 and 10:1 at 77 K.

MATERIALS AND METHOD

Materials

The starting reagents were $LiAlH_4$ (Sigma-Aldrich, ≥95%), $AlCl_3$ (Sigma-Aldrich, 99%) and LiCl (Sigma-Aldrich, 98%). Milling was performed in a SPEX 6850 cryomill using a custom-made 440c stainless steel rod milling canister held within two electromagnets in a chamber that is filled with liquid nitrogen. The small milling rod (32 g) is magnetically displaced 20 times per second with 1 g sample quantities placed within the canister between the end caps to provide a milling action at 77 K. LiCl was used as a buffer. The mixture of starting reagents with different LiCl: AlH_3 volume ratios (0.76:1, 2:1, 5:1 and 10:1) were milled for 30 minutes using a rod to powder mass ratio of 32:1 respectively. The sample was milled in a stepwise fashion (milled for 2 – 5 minutes and stopped for ~30 minutes incrementally) in an attempt to restrict the amount of heat build-up during milling.

Characterization

The chemical evolution of the reactant mixtures during processing AlH_3 was conducted using the X-Ray Diffraction (XRD) technique. This technique was performed using a BrukerD8 Advance diffractometer (Cu Kα radiation) with a 2θ range of 20°-100° using 0.02° steps with operating conditions of 40 kV and 40 mA. The sample was loaded into an XRD sample holder in an argon glovebox and sealed with a poly (methyl-methacrylate) (PMMA) airtight bubble to prevent oxygen/moisture contamination during data collection. The crystallite sizes were determined from an LVol-IB method that provides a good measure of the volume-weighted average crystallite size [17]. The structural parameters were refined from the diffraction data using Rietveld refinement in TOPAS (Bruker AXS, Karlsruhe, Germany) via a fundamental parameters approach.

RESULTS AND DISCUSSION

The mechanochemical reactions of the $3LiAlH_4 + AlCl_3 \rightarrow 4AlH_3 + 3LiCl$ proceeded to completion through the reduction of $LiAlH_4$ with $AlCl_3$ to formed AlH_3 nanoparticles as the reaction products. These AlH_3 nanoparticles were embedded within a buffer (LiCl) matrix. In order to understand the effect of buffer quantity on the particle size distribution and agglomeration, AlH_3 samples were synthesized via milling conditions as outlined in Table 1. It was expected that larger AlH_3 particles would be formed using low levels of buffer and smaller AlH_3 particles would be formed in samples with high buffer.

In order to understand the cryogenic synthesis, samples were first milled for 30 minutes (sample B) and 60 minutes (sample E) by using LiCl buffer (2:1 LiCl:AlH_3 volume ratio) respectively. Figure 1 shows the XRD patterns of the synthesized AlH_3. Both samples consist of peaks related to α-AlH_3, α'-AlH_3 and LiCl. Sample B contains α-AlH_3 and α'-AlH_3phases in a similar ratio. A decrease in α'-AlH_3 content and a new peak related to

Al were observed in the pattern of sample E. This shows that decomposition of AlH_3 to Al and H_2 has occurred during the milling process when the milling time was increased from 30 to 60 minutes.

Table 1: Overview of AlH_3 samples synthesis at 77 K details.

Sample	Rod to powder ratio	Milling time (min)	LiCl buffer (g)	Product volume ratio ($LiCl:AlH_3$)
A	32:1	30	0	0.76:1
B	32:1	30	0.46	2:1
C	32:1	30	0.74	5:1
D	32:1	30	0.86	10:1
E	32:1	60	0.46	2:1

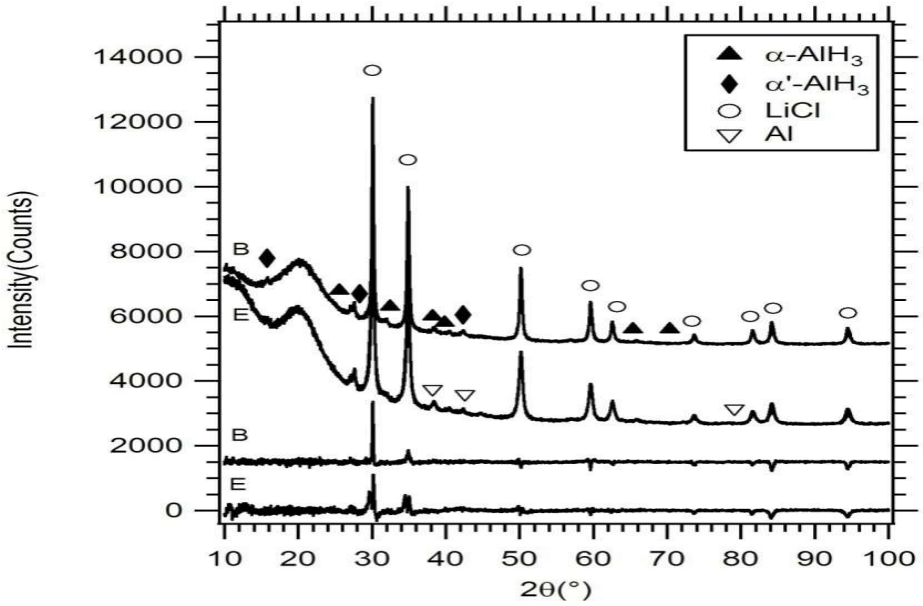

Figure 1. XRD patterns of synthesized AlH_3 milled for 30 minutes (sample B) and 60 minutes (sample E) by using 2:1 $LiCl:AlH_3$ volume ratio respectively.

Mechanochemical reactions of the $3LiAlH_4 + AlCl_3 \rightarrow 4AlH_3 + 3LiCl$ are moderately exothermic (ΔH=-213 kJ/mol), it provides more than enough energy for AlH_3 to decompose to Al and H_2 due to the low amount of energy required for decomposition (ΔH=+11.4 kJ/mol) [17]. At the same time, the milling process provides collision energy due to collision between reactant particles and balls inside the mill [12]. Therefore, the overall energy is generated from both the mechanochemical reaction and from the milling process itself. The addition of LiCl as a buffer, decreases the overall energy generation and lowers the reaction rate during mechanochemical reaction [12]. This is because during the mechanochemical reaction, the transferred energy into the reactant particles is reduced due to the presence of the buffer phase which absorbs some of the collision energy and heat energy [12]. As a result, no decomposition of AlH_3 to Al and H_2 is observed when the sample was milled for 30 minutes using LiCl buffer (2:1 $LiCl:AlH_3$ volume ratio). However, when the milling time was increased to 60 minutes, the total number of impacts will increase (produce high energy milling), which enables the AlH_3 phase transformation into α'-AlH_3 and enables AlH_3 decomposition into Al and H_2.

The AlH_3 and LiCl crystallite sizes were reduced when milling times increased from 30 minutes to 60 minutes (Table 3). During milling, deformation, fracture and welding of reactant particles occur repeatedly. Plastic deformation of the reactant particles initially occurs by reactant particles decomposing into sub-grains. After further milling, the sub-grains size decreases and nanometer size sub-grains are produced within each reactant particle. So, the reaction product will inherit the nanoscale microstructure of the reactant particles [19,20,21]. Upon increasing milling time, the total number of impacts will increase. Hence the reactant particles are subjected to higher mechanical induced energy, which results in particles decomposing into smaller sizes. Based on these results in order to produce nanoparticles of AlH_3 30 minutes milling time is preferred as a milling parameter for further investigation to limit the Al content of the samples but also allow for complete AlH_3 formation from reactants. Samples were cryogenically milled for 30 minutes with different LiCl:AlH_3 volume ratios of 2:1 (Sample B), 5:1 (Sample C) and 10:1 (Sample D) respectively. The addition of LiCl as a buffer restricts AlH_3 decomposition, prevents high Al yields and promotes AlH_3 nanoparticle formation.

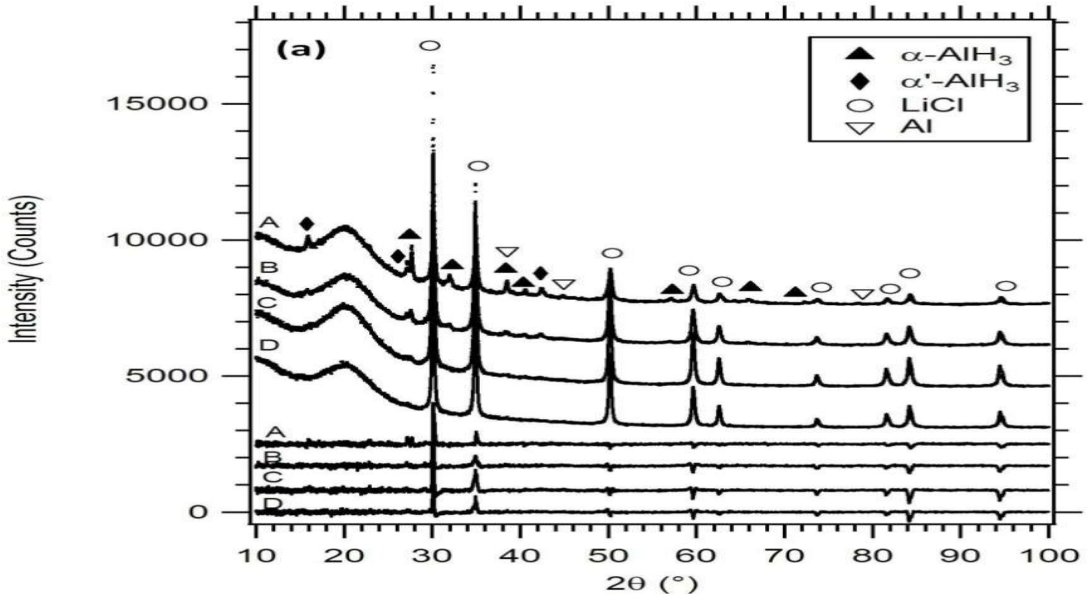

Figure 2. XRD patterns of synthesized AlH_3.

Figure 2 shows the XRD patterns of the synthesized AlH_3. Al peaks were not detected in all samples with buffer (Figure 2(a) samples B, C and D). The α'-AlH_3 peaks were not detected in sample C and both α-AlH_3 and α'-AlH_3 peaks were not detected in sample D. No other peaks are evident in the samples, which suggest that the reaction was completed.

Based on quantitative phase analysis (QPA) provided in Table 2, the crystalline wt.% of LiCl from Rietveld analysis is different from those calculated from expected yields. Rietveld analysis calculated wt.% values by assuming a sample content is 100% crystalline. For these AlH_3 samples, expected LiCl yields should result in 51.4 wt.%, 73.5wt.%, 87.4 wt.% and 93.2 wt.% LiCl for sample A, B, C and D. However, Rietveld results show crystalline LiCl consists of 60.1 ± 0.5 wt.%, 84.9 ± 0.6 wt.%, 96.5 ± 0.6 wt.% and 100 wt.% respectively. Since the crystalline LiCl content is larger from Rietveld analysis than the expected yields, an amorphous or poorly crystalline AlH_3 / Al phases may be formed during the mechanochemical reaction. This explains why AlH_3 / Al peaks were not evident in sample C and D. They could also just be broad due to their nanocrystalline nature and unobservable due to the low wt.% in the sample. This result is also consistent with a previous study of the synthesis of Y_2O_3 using the mechanochemical method, where no peaks corresponding to any yttrium phases were evident in the as-milled sample [22]. Heating of the washed sample resulted in the appearance of broadened diffraction peaks corresponding to Y_2O_3.

AlH_3 crystallite sizes decreased from 24.4 ± 1.3 nm (sample A), 15.0 ± 1.4 nm (sample B) and 8.7 ± 2.3 nm (sample C), for samples synthesised without using buffer and samples using LiCl:AlH_3 volume ratios of 2:1, 5:1 and 10:1 respectively (Table 3).

The addition of LiCl buffer led to a reduction of the synthesized AlH_3 crystallite size. In lower buffer content, the specific surface area of smaller particles is higher which provides higher driving force for particle coalescing and decreases their surface energy. On the other hand, because the volume fraction of the buffer phase is low, it cannot restrain the particle growth and agglomeration of the crystallites. However, in higher buffer content, the volume fraction of the buffer phase is sufficient to prevent particle agglomeration during the mechanochemical reaction by physical separation of the nanoparticles and therefore controls the particle size distribution [12].

Table 2: Rietveld results for phase composition calculated from XRD patterns in Figure 3. Mathematical fitting uncertainties are provided (2 standard deviations).

Sample	Phase composition (wt%)			
	α-AlH_3	α'-AlH_3	Al	LiCl
A	15.7 ±0.4	20.8 ±0.4	3.3 ± 0.2	60.1 ± 0.5
B	7.4 ± 0.4	7.6 ± 0.5	-	84.9 ± 0.6
C	3.4 ± 0.6	-	-	96.5 ± 0.6
D	-	-	-	100
E	7.2 ± 0.4	3.6 ± 0.4	3.3 ± 0.3	85.7 ± 0.6

Table 3: Rietveld results for crystallite size calculated from XRD patterns in Figure 3. Mathematical fitting uncertainties are provided (2 standard deviations).

Sample	Crystallite size (nm)			
	α-AlH_3	α'-AlH_3	Al	LiCl
A	24.4 ± 1.3	19.9 ± 1.2	26.3 ± 3.9	18.2 ± 0.2
B	15.0 ± 1.4	14.3 ± 2.2	-	21.1 ± 0.1
C	8.72 ± 2.3	-	-	25.6 ± 0.2
D	-	-	-	27.2 ± 0.2
E	14.9 ± 1.4	18.1 ± 5.1	7.5 ± 1.0	12.3 ± 0.1

CONCLUSIONS

Synthesis of AlH_3 by using mechanochemical reactions of the $3LiAlH_4 + AlCl_3$ with different LiCl:AlH_3 volume ratios at 77 K has been studied. The addition of LiCl as a buffer leads to the reduction of the synthesized AlH_3 crystallite size, restricting AlH_3 decomposition and preventing high Al yields. Quantitative Rietveld results suggest the presence of an amorphous AlH_3 phase in mechanochemically synthesized samples, which deserves further study to identify its structural properties.

ACKNOWLEDGEMENT

The author would like to thank the Government of Malaysia for funding and all personnel involved for their direct or indirect support to carry out this project.

REFERENCES

1. Fan Chen, Tian-Hao Yan, Sajid Bashir, Jingbo Louise Liu. 2022. Synthesis of nanomaterials using top-down methods. *Advanced Nanomaterials and Their Applications in Renewable Energy* ***(Second Edition)*** pp 37-60.
2. Josny Joy, Anand Krishnamoorthy, Ashish Tanna, Vishal Kamathe, Rupali Nagar and Sesha Srinivasan. 2022. Recent Developments on the Synthesis of Nanocomposite Materials via Ball Milling Approach for Energy Storage Applications. Appl. Sci. 12**(18)** pp 9312-9346
3. Tsuzuki, T.; McCormick, P. G. 2004. Mechanochemical synthesis of nanoparticles. *Journal of Materials Science* ***39*** pp 5143-5146.
4. Suryanarayana, C. 2001. Mechanical alloying and milling. *Progress in Materials Science* ***46*** pp 1-184.
5. Graetz, J.; Reilly, J. J.; Yartys, V. A.; Maehlen, J. P.; Bulychev, B. M.; Antonov, V. E.; Tarasov, B. P.; Gabis, I. E. 2011. Aluminum hydride as a hydrogen and energy storage material: Past, present and future. *Journal of Alloys and Compounds* 509 pp 5517-5528.
6. DeLuca, L. T.; Galfetti, L.; Severini, F.; Rossettini, L.; Meda, L.; Marra, G.; D'Andrea, B.; Weiser, V.; Calabro, M.; Vorozhtsov, A. B.; Glazunov, A. A.; Pavlovets, G. 2007. Physical and ballistic characterization of AlH_3-based space propellants. J. *Aerospace Science and Technology* **11** pp 18-25.
7. Brinks, H. W.; Istad-Lem, A.; Hauback, B. C. 2006. Mechanochemical Synthesis and Crystal Structure of α'-AlD_3 and α-AlD_3. *Journal of Physical Chemistry B* 110 pp 25833-25887.
8. Paskevicius, M.; Sheppard, D. A.; Buckley, C. E. 2009. Characterisation of mechanochemically synthesised alane (AlH_3) nanoparticles. *Journal of Alloys and Compounds 487* pp 370-376.
9. Sartori, S.; Istad-Lem, A.; Brinks, H. W.; Hauback, B. C. 2009. Mechanochemical synthesis of alane. *International Journal of Hydrogen Energy* **34** pp 6350-6356.
10. Lavernia, E. J.; Han, B. Q.; Schoenung, J. M. 2008. Cryomilled nanostructured materials: Processing and properties. *Materials Science and Engineering A* 493 pp 207-214.
11. Sartori, S.; Opalka, S. M.; Løvvik, O. M.; Guzik, M. N.; Tang, X.; Hauback, B. C. 2008. Experimental studies of α-AlD_3 and α'-AlD_3 versus first-principles modelling of the alane isomorphs. *Journal of Materials Chemistry* **18** pp 2361-2370.
12. Salari, M.; Rezaee, M.; Marashi, S. P. H.; Aboutalebi, S. H. 2009. The role of the diluent phase in the mechanochemical preparation of TiO_2 nanoparticles. *Powder Technology* 192 pp 54-57.
13. Dodd, A. C.; McCormick, P. G. 2002. Synthesis of nanocrystalline ZrO_2 powders by mechanochemical reaction of $ZrCl_4$ with LiOH. Journal of the European Ceramic Society 22 1823-1829.
14. McCormick, P. G.; Tsuzuki, T. 2002. Recent development in mechanochemical nanoparticle synthesis. *Materials Science Forum* 386-388 pp 377-388.
15. Hos, J. P.; McCormick, P. G. 2003. Mechanochemical synthesis and characterisation of nanoparticulate samarium-doped cerium oxide. *Scripta Materialia 48* pp 85-90.
16. Li, Y. X.; Chen, W. F.; Zhou, X. Z.; Gu, Z. Y.; Chen, C. M. 2005. Synthesis of CeO_2 nanoparticles by mechanochemical processing and the inhibiting action of NaCl on particle agglomeration. *Materials Letters* 59 pp 48-52.
17. Coelho, A. A., Topas User Manual, 3.0 ed. Bruker AXS GmbH, Karlsruhe, Germany, 2003.
18. M.Paskevicius, 2009. A Nanostructural Investigation of Mechanochemically Synthesised Hydrogen Storage Materials. Curtin University.

19. McCormick, P. G.; Tsuzuki, T.; Robinson, J. S.; Ding, 2001. Nanopowders Synthesized by Mechanochemical Processing. J. *Advanced Materials* **13** pp 1008-1010.

20. Tsuzuki, T.; Ding, J.; McCormick, P. G. 1997. *Physica B: Condensed Matter* 239 pp 378-387.

21. Tsuzuki, T.; McCormick, P. G. 1999. Mechanochemical synthesis of metal sulphide nanoparticles *Nanostructured Materials* **12** pp 75-78.

22. Dodd, A. C., & McCormick, P. G. 2004. Synthesis of Nanocrystalline Yttrium Oxide Powders by Mechanochemical Processing. *Journal of Metastable and Nanocrystalline Materials,* **20-21** pp *319–324.*